

A mathematical description is given for crystallization and cooling for drops of a one-component liquid during granulation in an ascending coolant flow. An algorithm is proposed.

In some methods of calculating granulation for liquid drops [1-3] such as ammonium nitrate, carbamide, NP fertilizers, and sulfur, where coolant flows in a granulation tower or column, no allowance is made for the initial supercooling or for the relationship between the temperature at the phase front, which is related to the linear rate of crystal growth, or for the heat loss to the coolant, which varies over the surface of a drop, although it has been demonstrated by experiment that these factors are relevant [1, 4-6].

We give below a model and a method of using it with these factors. It is assumed that a drop is initially spherical and the rate of heat loss to the coolant is variable over the surface, being represented by standard relationships [7] for single drops, with serial crystallization occurring with a prominent phase boundary and with pronounced boundaries for the modification transitions. It is assumed that the density difference between the liquid and solid results in an enlarging shrinkage cavity at the center, whose shape is determined as far as possible from the conditions for minimum surface energy. The channel joining the shrinkage cavity to the atmosphere is taken as cylindrical and having 0.15 of the granule diameter, which corresponds to that observed in crystallized granules. The temperature dependence of the density means that there is also distributed shrinkage in the crystalline framework in the form of micropores and cracks. The shrinkage volume is calculated at each time step from the mass conservation conditions. With various substances (here carbamide and sulfur), an initial supercooling  $t_p - t_s$  precedes the crystallization [4-6], which is related to the onset of heterogeneous nucleation in the surface layers, which has been identified by experiment [4, 6, 8, 9]. The speed  $W_p$  of the polycrystalline front is dependent on the supercooling  $(t_p - t_{ij}^{\phi})$ . We have used the experimental data of [8, 10] on the crystallization kinetics of carbamide and sulfur in capillaries on the basis of the temperature discrepancy between the phase front and the thermostat. The specific coolant flow was calculated from standard relationships [11] for the interaction of a continuous phase with a jet of a dispersed one.

The following equations describe the heat transfer in the phases, at the interphase boundaries, and at the outer boundary of drops in the polydisperse mixture:

$$\frac{\partial}{\partial r_j} \left[ \lambda_i \frac{\partial t_{ij}}{\partial r_j} \right] + \frac{2\lambda_i}{r_j} \frac{\partial t_{ij}}{\partial r_j} + \frac{\text{ctg } \varphi_j}{r_j^2} \lambda_i \frac{\partial t_{ij}}{\partial \varphi_j} + \frac{1}{r_j^2} \frac{\partial}{\partial \varphi_j} \times$$

$$\times \left[ \lambda_i \frac{\partial t_{ij}}{\partial \varphi_j} \right] - C_i \rho_i \frac{\partial t_{ij}}{\partial \tau} = 0, \quad i=0, 1, 2, \dots, I; \quad j=1, 2, \dots, J. \quad (1)$$

The initial conditions are

$$t_{ij} = t_{0\text{in}} = \text{const}, \quad 0 \leq r_j \leq R_j; \quad \varphi_{j,1} = R_j + 0; \quad \varphi_{j,2} = 0; \quad t_c = t_c(H). \quad (2)$$

The conditions at the boundary of the shrinkage cavity are

$$\frac{\partial t_{ij}}{\partial n_j} = 0,$$

where

$$\begin{aligned}
 v_{s_j}(\tau) &= v_{1j}(\tau) \frac{\rho_1(t_f) - \rho_{0in}}{\rho_{0in}} \frac{F_{s_j}}{v_{s_j}} \rightarrow \left( \frac{F_{s_j}}{v_{s_j}} \right)_{\min}; \\
 v'_{s_j}(\tau) &= \frac{v_{1j}(\tau) \langle \rho_1 \rangle + v_{0j}(\tau) \langle \rho_0 \rangle - v_{p0in}}{\langle \rho_1 \rangle}, \\
 \langle \rho_1 \rangle &= \frac{1}{v_{1j}} 2\pi \int_{r_{pj}}^{R_j} \int_0^\pi \rho_1(r_j, \varphi_j) r_j^2 \sin \varphi_j d\varphi_j dr_j; \\
 \langle \rho_0 \rangle &= \frac{1}{v_{0j}} 2\pi \int_{r_{yj}}^{r_{pj}} \int_0^\pi \rho_0(r_j, \varphi_j) r_j^2 \sin \varphi_j d\varphi_j dr_j;
 \end{aligned} \tag{3}$$

and those at the phase boundary are

$$t_{ij}^p = t_{i+1j}^p, \tag{4}$$

$$\lambda_{i+1} \frac{\partial t_{i+1j}}{\partial n_j} - \lambda_i \frac{\partial t_{ij}}{\partial n_j} = L_p \rho_i \omega_{pj}, \tag{5}$$

$$\omega_{pj} = \begin{cases} 0 & \text{at } r_{pj} \equiv R_j + 0 \text{ and } t_{ij} > t_{si}, \\ f_2 [t_p - t_{ij}^p] & \text{at } r_{pj} < R_j; \end{cases} \tag{6}$$

and at the outer boundary of the drop

$$\alpha_{cj} [t_{ij} - t_c(\tau)] = -\lambda_i \frac{\partial t_{ij}}{\partial n_i}. \tag{7}$$

The local values of the distributed porosity in the rigid crystalline crust  $\psi(r_j, \varphi_j)$  at a given instant are defined by

$$\psi(r_j, \varphi_j) = \frac{\rho_1(r_j, \varphi_j) - \rho_1(t_p)}{\rho_1(r_j, \varphi_j)}.$$

The heat balance between the crystallizing granules and the coolant in an elementary part of the apparatus of height  $dH$  takes the form

$$\int_0^\infty \int_0^\pi \frac{1}{R_j} \alpha_{cj} [t_{ij} - t_c(\tau)] \sin \varphi_j d\varphi_j \frac{1}{W_j} \xi_p(R_j) dR_j dH = -\frac{2}{3} GC_c \rho_0 dt_c. \tag{8}$$

System (1)-(8) is closed by

$$W_j = W_p - \frac{W_c}{\varepsilon}, \tag{9}$$

where

$$\frac{\rho_0(1-\varepsilon)}{\rho_c} = \frac{W_c}{G} \int_0^\infty \xi_p(R_j) \frac{dR_j}{W_p - \frac{W_c}{\varepsilon}}; \quad H = \int_0^{\tau(R_j)} W_j d\tau.$$

System (1)-(9) can be solved by numerical methods such as finite differences. One approximates (1)-(9) by an implicit finite-difference analog nonlinear with respect to the values of the net function at a given time step:

$$(C\rho)_i^{s+1} \Lambda_\tau T^{s+1} = \lambda_i^{s+1}(T) \Lambda_{rj} T^{s+1} + \lambda_i^s(T) \Lambda_{\varphi j} T^s. \tag{10}$$

The initial conditions are

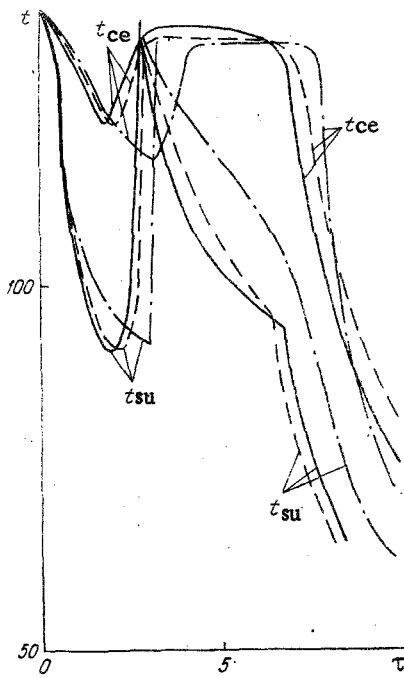


Fig. 1. Variation in the temperature at the center  $t_{ce}$  and at the surface  $t_{su}$  in a granule; the solid lines are the results from high-speed thermal analysis, while the dashed and dot-dash lines are calculations with variable and constant  $\alpha_c$  at the surface of a granule correspondingly ( $R = 1.3$  mm,  $t_c = 25^\circ\text{C}$ ,  $t_0 = 137^\circ\text{C}$ ,  $W_p = 2$  m/sec),  $t$ ,  $^\circ\text{C}$ ,  $\tau$  in sec.

$$T = t_0 = \text{const}, \quad r_{pj} \equiv R_j + 0; \quad r_{sj} \equiv 0; \quad T_c = t_c(H). \quad (11)$$

The boundary conditions are

$$\Lambda'_{nj} T^{s+1} = 0, \text{ where } v_{yj}^{s+1} = v_{1j}^{s+1} \frac{\rho_1(t_p) - \rho_{0in}}{\rho_{0in}}, \quad \frac{F_{sj}}{v_{sj}} \rightarrow \left( \frac{F_{sj}}{v_{sj}} \right)_{\min}; \quad (12)$$

$$v_{sj}^{s+1} = \frac{v_{1j}^{s+1} \langle \rho_1 \rangle + v_{0j}^{s+1} \langle \rho_0 \rangle - v \rho_{0in}}{\langle \rho_1 \rangle};$$

$$\langle \rho_{1,0} \rangle = \frac{1}{v_{1,0j}} 2\pi \sum_{(\Delta r_j)} \sum_{(\Delta \varphi_j)} \rho_{1,0}(r_j, \varphi_j) r_j^2 \sin \varphi_j \Delta \varphi_j \Delta r_j; \quad (13)$$

$$T_i^{s+1} = T_{i+1}^{s+1};$$

$$\lambda_{i+1}^{s+1}(T) \Lambda'_{rj} T^{s+1} - \lambda_i^{s+1}(T) \Lambda'_{rj} T^{s+1} = L_p \rho_i \frac{\Delta r_{pj}^{s+2}}{\Delta \tau}; \quad (14)$$

$$\frac{\Delta r_{pj}^{s+2}}{\Delta \tau} = \begin{cases} 0 & \text{for } r_{pj} \equiv R_j + 0 \text{ and } T^{s+1} > t_{si}, \\ f_2 [t_p - T_i^{s+1}] & \text{for } r_{pj} < R_j; \end{cases} \quad (15)$$

$$\alpha_{cj} [T_i^{s+1} - T_c^{s+1}] = -\lambda_i^{s+1}(T) \Lambda'_{nj} T^{s+1}. \quad (16)$$

System (10)-(16) is closed by

$$\sum_{i=1}^L \sum_{j=1}^J \sum_{x=1}^X \frac{1}{R_j} \alpha_{cxj} [T_i^{s+1} - T_c^{s+1}] \sin \varphi_{xj} \Delta \varphi_{xj} \frac{1}{W_j} \Delta \xi_p(R_j) \Delta h_i = -\frac{2}{3} GC_c \rho_0 \sum_{i=1}^L \Delta T_{cl}^{s+1}, \quad (17)$$

where

$$\Delta h = \int_{\Delta \tau(R_j)} W_j d\tau, \quad H = \sum_{i=1}^L \Delta h_i; \quad (18)$$

$$W_j = W_p - \frac{W_c}{\varepsilon},$$

where

$$\frac{\rho_0(1-\varepsilon)}{\rho_c} = \frac{W_c}{G} \sum_{j=1}^J \Delta \xi_p(R_j) \frac{\Delta R_j}{W_p - \frac{W_c}{\varepsilon}}.$$

The nonlinear difference analog (10)-(18) of (1)-(9) was solved by means of the algorithm proposed in [12] involving the use of mobile nodes in the cells of the spatial net through which the crystallization and phase-transition fronts pass. Allowance is made for the positions of the phase boundaries, the temperatures at them, the temperature patterns in the phases, the shapes and sizes of the shrinkage cavities, and the parameters described by (18) derived from the previous iteration  $s$  in order to calculate the distribution of the net functions in the phases in iteration  $s+1$  by successive solution involving fitting [13] the one-dimensional equations of (10) along all the axes  $r$ . The resulting data are used with (13) and (14) to determine the phase-boundary displacements, while (15) gives the temperatures at them, and then one calculates the volume of the crystalline phase in a drop, and from (12) derives the volume  $v_{sj}^{s+1}$  of the shrinkage cavity, with the shape (as far as possible) taken as spherical, and in the subsequent calculations taken such that  $F_{sj}/v_{sj} \rightarrow \min$ . This condition is realized by selection over the sectors such that the ratio of the total increment in the surface of the shrinkage cavity by sectors to the volume is minimal. In that way, one determines the coordinates of the boundary to the shrinkage cavity in each sector, as well as the shape and dimensions as a whole. As we know the temperature distribution in the drop and the temperature dependence of the phase densities, one can use the conditions for conservation of the crystalline-phase volume with (12) to calculate the porosity of the crystalline framework. These calculations are performed at a given time step for all fractions in the polydisperse mixture. If the calculated values do not coincide with the specified ones within the specified accuracy, the iteration is repeated. When one implements nonlinear difference analogy with this algorithm, transverse fitting (on the  $\varphi$  axis) is eliminated by comparison with the additive and factorization schemes of [13]. The convergence of the iteration can be accelerated by standard methods [14]. The errors in the solutions have been evaluated by Runge's method involving varying the space and time steps by factors of two and four. With an accuracy sufficient for engineering calculations (error less than 5%), the time step was chosen such that the region was split up into ten sectors in  $\varphi$  with ten nodes in  $r$ , while the polydisperse mixture was divided into five fractions by  $R_j$ . In 3-4 iterations with only the use of halving, the discrepancies in  $r_{fj}$  and the temperature pattern did not exceed 3%. The thermophysical parameters were taken from the reference literature [4, 5].

In the particular case where the heat loss rate is assumed constant over the surface, (1)-(9) imply a description that has been used by ourselves and others to calculate granulation for molten ammonium nitrate [1, 15], carbamide [2, 10], sulfur [8, 9], and other substances [3] in towers and columns employing liquid coolants [12]. However, it has been shown [12] that that assumption gives marked distortion for ammonium nitrate as regards the size and shape of the shrinkage cavity, the temperature pattern, and the positions of the phase boundary and the boundaries between the modifications. In relation to carbamide and sulfur, it is necessary to incorporate the initial supercooling and the dependence of the temperature at the phase front on the linear growth rate. As an example, we give calculations on the crystallization of carbamide in towers.

One can compare the calculations with variable and constant transfer rates with results from high-speed thermal analysis [4], which shows that there is better agreement in the

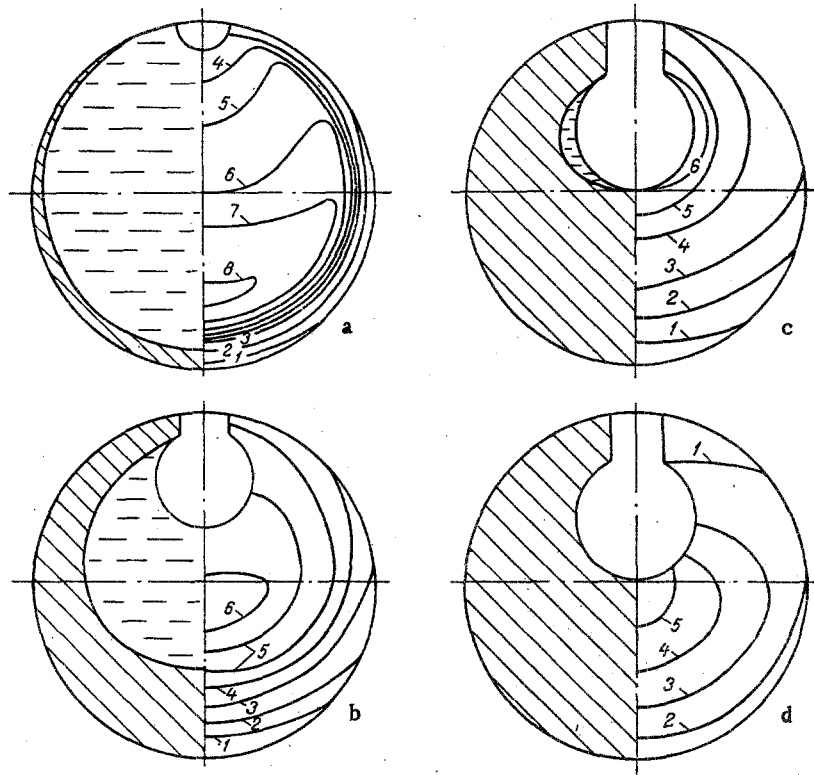


Fig. 2. Positions of crystallization and shrinkage-cavity fronts in a granule at various instants (left) and of temperature patterns (right): a)  $\tau = 1.5$  sec; 1)  $128^\circ\text{C}$ , 2) 131, 3) 130, 4) 126, 5) 124, 6) 122, 7) 120, 8) 118; b)  $\tau = 3.0$  sec; 1)  $110^\circ\text{C}$ , 2) 115, 3) 120, 4) 125, 5) 130, 6) 129; c)  $\tau = 5.0$  sec: 1)  $90^\circ\text{C}$ , 2) 100, 3) 105, 4) 125, 5) 130 c) 132, d)  $\tau = 7.0$  sec; 1)  $50^\circ\text{C}$ , 2) 55, 3) 60, 4) 65, 5) 70 ( $R = 1$  mm,  $t_{\text{cin}} = 20^\circ\text{C}$ ,  $t_0 = 137^\circ\text{C}$ ,  $G = 20$  (kg/h of coolant)/ (kg/h of product),  $W_p = 0.44$  m/sec, and  $W_{\text{in}} = 2$  m/sec).

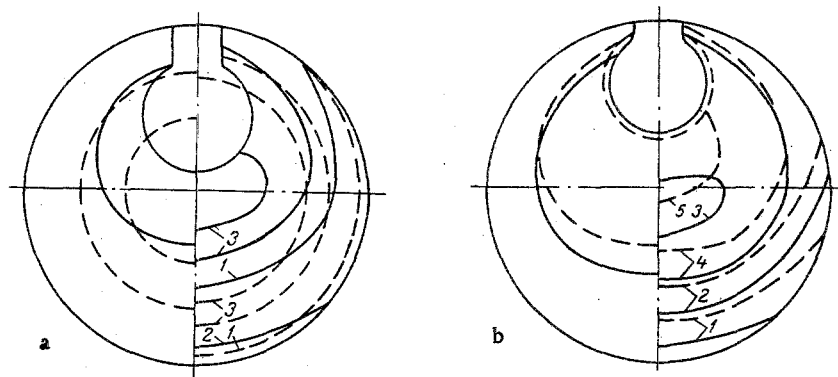


Fig. 3. Calculation results (conditions as in Fig. 2): a) solid line for variable rate of heat transfer to coolant, dashed line for rate constant over the surface,  $\tau = 4$  sec: 1)  $120^\circ\text{C}$ , 2) 100, 3) 130; b) solid lines by calculations with allowance for the initial supercooling and  $w_p = f[t_p - t_{ij}^p]$  dashed lines calculations without allowance for crystallization kinetics,  $\tau = 3$  sec: 1)  $110^\circ\text{C}$ , 2) 120, 3) 129, 4) 130, 5) 136.

first case (Fig. 1).

As examples, we show individual calculated projections of the phase boundaries and shrinkage cavity, as well as the isotherms at various instants, which indicate the crystallization dynamics and the formation of a shrinkage cavity in a droplet in a polydisperse

mixture in a granulation tower (Fig. 2). The low nucleation rate for carbamide means that the droplets at first become very much supercooled (Figs. 1 and 2): experiment shows [4], which we have confirmed for various droplet sizes and cooling rates with Kazakova's high-speed thermograph, that on attaining  $t_s \approx 90^\circ\text{C}$  at the surface, crystallization begins; the heat loss from the phase front to the coolant and into the supercooled liquid means that the crystallization rate is initially very high, and the crystalline crust grows more rapidly than in granulating ammonium nitrate with  $\alpha_c$  variable [12]. The high rate and the high latent heat of crystallization for carbamide mean that the supercooling is rapidly eliminated (Figs. 1 and 2), and the probability of bulk crystallization is reduced, as is that of instability at the phase boundary.

The crystalline crust brings together the edges of the depression formed at the rear of the drop on account of the opposing flow of air, and then the shrinkage cavity extends into the drop and takes a form providing minimal specific surface (Fig. 2). At the end, the volume of the shrinkage cavity is about 4.5%, while the volume of the external shrinkage (reduction in droplet size due to density difference between the liquid and crystalline phase when not all the surface is covered by the crystalline crust) is on average 3% of the granule volume for each fraction, which agrees well with results obtained by mercury porometry and by pycnometric methods as well as by observation of sectioned granules under the microscope. It has previously been found [12] that there is good agreement between an analogous calculation and experiment for ammonium nitrate granules. Qualitative principles have been formulated [16] on the formation of shrinkage cavities, obedience to which enables one to obtain ammonium nitrate and carbamide granules with smooth surfaces (without channels linking the shrinkage cavities to the atmosphere), which are suitable for encapsulation in polymers [12, 16].

If one ignores the variable heat transfer, one distorts the dynamic expansion of the crystalline phase, although the error in determining the complete crystallization time is small. In that case, one cannot calculate correctly the size and position in the granule of the shrinkage cavity or the position of the crystallization boundaries and the temperature patterns (Fig. 3a).

If one assumes that the polydisperse mixture is in fact monodisperse, one underestimates the crystallization times for the large fractions  $R_j = 1.0\text{--}1.5$  mm by 10–15% with specific coolant flows  $G \geq 10$ . At smaller  $G$  (such as tend to be used in making fertilizers), this error increases substantially.

Ignoring the initial supercooling and the dependence of the linear growth rate on supercooling reduces the complete crystallization time by 15–20% for carbamide or by 60–100% for sulfur, the exact cooling conditions and granule size affecting the values. Figure 3b shows also that the temperature patterns and the positions of the crystallization boundaries are distorted.

This aspect must be borne in mind in detailed calculations on granulation in a coolant flow.

#### NOTATION

$C$ , heat capacity;  $F_s$ , surface of shrinkage cavity,  $\alpha_{cj}$ , known [7] function for heat-transfer coefficients of single particles;  $f_2$ , supercooling dependence of the linear growth rate of the polycrystalline front for carbamide [10] and sulfur [8];  $W_p$ , known function for velocity of falling particles injected at an angle to the horizon [17];  $W_c, G$ , known [11] functions for velocity of solid phase and specific flow rate of coolant in injection jet;  $G$ , coolant specific flow rate;  $G_0$ , melt flow rate;  $H$ , height of tower;  $L_p$ , heat of phase conversion;  $n$ , normal to isotherm;  $R, r, r_p, r_s$ , drop radius, current radius, phase conversion radius, and radius of shrinkage cavity, respectively;  $T$ , value of net function;  $t$ , temperature,  $t_p$ , thermodynamic temperature of phase transition;  $t_s$ , initial drop supercooling [6, 9, 10];  $v, v_0, v_1, v_s, v_s^i$ , volumes of drop, melt, crystalline phase, shrinkage cavity, and distributed shrinkage;  $w_p$ , normal velocity of phase boundary;  $W_j, W_i$ , velocity of fraction  $j$  relative to apparatus walls and of entry from granulator;  $j, J$ , fraction number and number of fractions;  $s$ , iteration number;  $\alpha$ , heat transfer coefficient;  $\Delta_r, \Delta_\varphi$ , difference analogs of heat-conduction operators in spherical coordinates  $r$  and  $\varphi$ ;  $\Delta'$ , difference analog of the first derivative;  $\lambda$ , thermal conductivity;  $\rho$ , density;  $\varphi$ , angle reckoned from the flow axis;  $\tau$ , time;  $\xi_p(R_j)dR_j$ , fraction of size  $R_j$  in mixture;  $\epsilon$ , porosity;  $\Delta$ , finite increment. Subscripts: 0, melt; 1, 2, ..., crystalline phases of modifications 1, 2, ...; in, initial; t, total, c, medium (coolant); s, shrinkage; p, phase.

## LITERATURE CITED

1. V. M. Olevskii (ed.), Ammonium Nitrate Technology [in Russian], Khimiya, Moscow (1978).
2. A. M. Vainberg, V. I. Mukosei, and V. S. Beskov, "Simulating granulation from the melt and application in designing granulation towers," Trudy GIAP, No. 40, 48-58 (1976).
3. M. E. Ivanov, V. M. Lindin, and K. M. Zakharova, "The cooling of carbamide and nitroamophos granules in tower granulation," Trudy GIAP, No. 49, 39-47 (1979).
4. E. A. Kazakova, Granulation and Cooling of Nitrogen Fertilizers [in Russian], Khimiya, Moscow (1980).
5. V. M. Borisov, "The physicochemical principles of droplet flotation in sulfur suspensions," Trudy GIGKhS, No. 6, 287-305 (1960).
6. A. V. Taran, N. I. Gel'perin, and G. I. Lapshenkov, "A study of molten sulfur crystallization in granulation towers by electrical simulation," Izv. Vyssh. Uchebn. Zaved., Khim. Tekhnol., 22, No. 6, 753-757 (1979).
7. T. R. Galloway and B. H. Sage, "Thermal and material transfer from spheres: prediction of local transport," Int. J. Heat Mass Transf., 11, 539-549 (1968).
8. A. V. Taran, N. I. Gel'perin, V. M. Larovskii, and G. I. Lapshenkov, "A study of sulfur granulation in a countercurrent of air by electrical simulation," Chemistry and Technology of Inorganic Materials (Intercollegiate Collection, Moscow Institute of Chemical Engineering and Moscow Institute of Fine Chemical Technology) [in Russian], No. 1, Moscow (1978), pp. 111-116.
9. A. L. Taran, A. V. Taran, and G. I. Lapshenkov, "Accelerating the granulation of sulfur in towers," TOKhT, 16, No. 4, 559-563 (1982).
10. T. I. Shcherbatykh, N. I. Gel'perin, A. V. Taran, and G. I. Lapshenkov, "A study of carbamide crystallization in granulation towers by electrical simulation," Chemistry and Technology of Inorganic Materials (Intercollegiate Collection, Moscow Institute of Chemical Engineering and Moscow Institute of Fine Chemical Technology) [in Russian], Vol. 8, No. 1, Moscow (1978), pp. 128-132.
11. M. E. Ivanov, "Granule dispersal and sheathed flow of the continuous medium with the two moving from a single source," TOKhT, 17, No. 4, 551-554 (1983).
12. A. L. Taran and Yu. M. Kabanov, "Solidification of nitrogen-fertilizer granules with heat-transfer rates unevenly distributed over the surface," TOKhT, 17, No. 6, 759-766 (1983).
13. A. A. Samarskii, Theory of Difference Schemes [in Russian], Nauka, Moscow (1983).
14. J. M. Ortega and W. C. Rheinboldt, Iterative Solution of Nonlinear Equations in Several Variables, Academic Press (1970).
15. N. I. Gel'perin, G. I. Lapshenkov, and A. L. Taran, "A study of ammonium nitrate granulation in towers by electrical simulation," Khim. Prom., No. 3, 205-209 (1977).
16. Yu. M. Kabanov, A. V. Taran, and A. L. Taran, "Granulating ammonium nitrate in liquid coolants to produce granules suitable for effective encapsulation," Proceedings of the Second All-Union Conference [in Russian], Sumskoi Filial KhPI, Sumy (1982), Part 2, pp. 34-35.
17. M. E. Ivanov and A. B. Ivanov, "A solution for the general case of two-dimensional motion of granules under gravity," Inzh.-Fiz. Zh., 28, No. 1, 119-123 (1975).